PROCEEDINGS, Thirty-Second Workshop on Geothermal Reservoir Engineering
Stanford University, Stanford, California, January 22-24, 2007
SGP-TR-183

STRESS AND PORE PRESSURE DISTRIBUTION AROUND A PRESSURIZED, COOLED CRACK IN LOW PERMEABILITY ROCK

A. Ghassemi

University of North Dakota
P.O. Box 8358
Grand Forks, ND, 58202, USA
e-mail: ahmadghassemi@mail.und.edu

ABSTRACT

Thermoelastic and poroelastic stresses associated with water injection and hydraulic fracture stimulation can result in rock failure in the vicinity of the main fracture leading to permeability change and enhanced micro-seismicity. The monitoring and analysis of the micro-seismicity is used to better understand stimulation outcomes, and this process can benefit from a stress/failure analysis. A coupled displacement discontinuity method is used in this paper to study the stress and pore pressure changes around a cooled fracture in low-permeability rock, to investigate their contribution to rock failure and seismicity. Simulations of a uniformly cooled crack indicate that cooling introduces a transient reduction in pore pressure that has a stabilizing effect with respect to shear failure of intact rock and slip on pre-existing cracks. Thermally-induced stresses also cause formation of new secondary cracks that can generate micro-seismic events. Regions of enhanced shear stress with higher potential for shear failure are also observed near the crack ends and off the main fracture plane. The distribution of the stress and pore pressure fields vary with time, resulting in a time-dependent rock failure distribution.

INTRODUCTION

The production of geothermal energy from dry and low permeability reservoirs is achieved by water circulation in natural and/or man-made fractures, and is often referred to as enhanced or engineered geothermal systems (EGS). Two or more wells are drilled into the reservoir to intersect permeable fractures, and cold water is injected into one part of the well system and hot water/steam is recovered from the other. Cold water injection perturbs the in-situ stress state within the reservoir leading to fracture initiation and/or activation of discontinuities such as faults and joints which is often manifested as multiple microseismic events. Detection and interpretation of microseismic events using downhole receiver arrays (e.g., Brady et al., 1994; Warpinski et al., 1996) can be monitored and analyzed to provide useful information on the stimulated zone, fracture growth, and geometry of the geological structures and the in-situ stress state (Warpinski et al., 2001; Guiterez, 2003; Pine, 1984**).** Micro-seismic events are believed to be associated with rock failure in shear, and shear slip on new or pre-existing fracture planes (Peasron, 1981). The generated microseismic signals contain information about the sources of energy that can be used for understanding the hydraulic fracturing process (e.g., Foulger et al., 2006; Vandamme et al., 1994; Warpinski, et al., 1997). Recent developments allow identification and interpretation of mode 1 crack propagation (Foulger at al., 2004) also. Effective interpretation of micro-seismicity can benefit from the knowledge of the hydro-thermo-mechanical mechanisms associated with injection in the reservoir, and the resulting stress variations that play a key role in rock failure around the main hydraulic fracture. These include the stresses due to the opening of a hydraulic fracture, and thermoelastic and poroelastic stresses due to rock cooling and fluid leak-off into the rock mass.

In this paper we investigate the stress and pore pressure changes around a fracture. In general, an injection-induced fracture problem consists of three components: (1) fluid flow and heat transport within the fracture, (2) fluid flow in the matrix, (3) conductive and advetcive heat transport in the matrix, and (4) fracture propagation. Solutions to the problem involving the first three parts have been presented (Nygren & Ghassemi, 2006; Nygren at al., 2005). The fracture propagation aspect can be treated using e.g., a coupled displacement discontinuity method. The current porothermoelastic DD method is based on a conduction-limited, fully coupled model. However, it can be used to calculate the stress and failure distribution in the rock matrix around a cooled and pressurized stationary crack in low-permeability geothermal reservoirs.

THEORY OF PORO-THERMOELASTICITY

Thermo-poroelastic stresses can be treated quantitatively within the framework of non-isothermal poroelastic theory, or poro-thermoelasticity. The relevant equations are:

Constitutive Equations:

$$\Delta\varepsilon_{ij} = \frac{\Delta\sigma_{ij}}{2G}, i \neq j \quad (1)$$

$$\Delta\varepsilon_{kk} = \frac{\Delta\sigma_{kk}}{3K} + \frac{\alpha\Delta p}{K} + \beta_s^{'}\Delta T \quad (2)$$

$$\sigma_{ij} = 2G\varepsilon_{ij} + \frac{2G\nu}{1-2\nu}\varepsilon\delta_{ij} - \alpha p\delta_{ij} + K\beta_s^{'}T\delta_{ij} \quad (3)$$

$$\Delta\zeta = \frac{\alpha}{3K}\Delta\sigma_{kk} + \frac{\alpha\Delta p}{BK} - \phi_0\left(\beta_f - \beta_s^{''}\right)\Delta T \quad (4)$$

Equilibrium equations:

$$\sigma_{ij,j} = 0 \quad (5)$$

Darcy's law:

$$v_i = -\frac{k}{\eta}p_{,i}\ ;\ w_i = \int_0^t v_i \quad (6)$$

Continuity equations:

$$\frac{\partial\zeta}{\partial t} + q_{i,j} = 0 \quad (7)$$

Fourier law:

$$q_i^T = -k^T T_{,i}\ ;\ h_i = \int_0^t q_i^T \quad (8)$$

where σ_{ij} denotes the components of the total stress tensor, ζ is the variation of the fluid content per unit volume of the porous material, and ε_{ij} are the components of the strain tensor. The constant *K* is the rock's bulk modulus; *B* is Skempton's pore pressure coefficient; α is Biot's effective stress coefficient; $\beta_s^{'}$ is the volumetric thermal expansion coefficient of the bulk solid under constant pore pressure and stress; and $\beta_s^{''}$ and β_f represent volumetric thermal expansion coefficients of the solid matrix and the pore fluid, respectively. The former, $\beta_s^{''}$, reflects the phenomena engendered by the internal pore geometry and the stress fields that are caused by a temperature change (Palciauskas and Domenico, 1982); it may be considered equal to $\beta_s^{'}$ (henceforth denoted by β_s) if the change in temperature is not expected to change porosity, ϕ_o. The above equations can be combined to yield a set of field equations:

$$G\nabla^2\mathbf{u} + \left(\frac{G}{1-2\nu}\right)\nabla\left(\nabla\cdot\mathbf{u}\right) - \alpha\nabla\mathbf{p} - \beta_s K\nabla T = \mathbf{0} \quad (9)$$

$$\frac{1}{M}\frac{\partial p}{\partial t} = \frac{k}{\eta}\nabla^2 p - \alpha\frac{\partial\left(\nabla\cdot\mathbf{u}\right)}{\partial t} + d\frac{\partial T}{\partial t} \quad (10)$$

$$\frac{\partial T}{\partial t} = c^T\nabla^2 \quad (11)$$

$$M = \frac{2G\left(\nu_u - \nu\right)}{\alpha^2\left(1-2\nu\right)\left(1-2\nu_u\right)}$$

where d= $\alpha\beta_s + \phi\left(\beta_f - \beta_s\right)$; $\kappa = k/\eta$, in which *k* is dynamic permeability and η is the fluid viscosity; k^T is the thermal conductivity and c^T is the thermal diffusivity. *G* is shear modulus and M is Biot's modulus. It should be noted that for most rocks, heating/cooling produces thermal stresses and changes in pore pressure, but stress and pressure changes do not significantly alter the temperature field. Thus, the latter is not coupled to the equations for the pore pressure and solid displacements. Also, note that convective heat transport is neglected. This is justified for rocks of interest that have a low permeability.

METHOD OF ANALYSIS

The injection-induced fracturing problem and the resulting stress and pore pressure in its surrounding, consist of heat and fluid transport in the fracture and the reservoir matrix, and fracture propagation. In general, this coupled problem is not amenable to analytical treatment and needs to be solved numerically. An iterative semi-analytical solution is possible for a simplified version of this problem suitable for petroleum reservoirs (e.g., Perkins & Gonzales, 1981).

This work focuses on the impact of a cooled fracture on stress and pore pressure in eth reservoirs. The fracture is considered to be stationary, and is modeled using a two-dimensional displacement discontinuity (DD) boundary element technique. The DD method is particularly suitable for studying faults and joints and has been used to study fracture problems in plane

strain (Crouch and Starfield, 1983; Ghassemi and Zhang (2006) as well as in 3D (Ghassemi and Roegiers, 1996). The displacement discontinuity (DD) boundary element method utilizes singular solutions for a point fluid and heat source along with a point DD. For the sake of brevity, the details of the formulation are not presented. The interested reader is referred to (Ghassemi and Zhang, 2006).

The thermo-poroelastic problems can be modeled by distributing displacement discontinuity and fluid and heat sources on the boundary surface and requiring that the superposition of their effects satisfy the prescribed boundary conditions. Then a set of boundary integral equations are obtained for induced stresses, pore pressure and temperature:

$$\sigma_{ij}(\mathbf{x},t)=\int_0^t\int_\Gamma\left\{\begin{array}{l}\sigma_{ijk}^{id}(\mathbf{x},\boldsymbol{\chi};t-\tau)D_k(\boldsymbol{\chi},\tau)\\+\sigma_{ij}^{is}(\mathbf{x},\boldsymbol{\chi};t-\tau)\phi(\boldsymbol{\chi},\tau)\\+\sigma_{ij}^{ih}(\mathbf{x},\boldsymbol{\chi};t-\tau)\varphi(\boldsymbol{\chi},\tau)\end{array}\right\}d\Gamma(\boldsymbol{\chi})d\tau \qquad (12)$$

$$p(\mathbf{x},t)=\int_0^t\int_\Gamma\left\{\begin{array}{l}p_k^{id}(\mathbf{x},\boldsymbol{\chi};t-\tau)D_k(\boldsymbol{\chi},\tau)\\+p^{is}(\mathbf{x},\boldsymbol{\chi};t-\tau)\phi(\boldsymbol{\chi},\tau)\\+p^{ih}(\mathbf{x},\boldsymbol{\chi};t-\tau)\varphi(\boldsymbol{\chi},\tau)\end{array}\right\}d\Gamma(\boldsymbol{\chi})d\tau$$

$$T(\mathbf{x},t)=\int_0^t\int_\Gamma\left\{T^{ih}(\mathbf{x},\boldsymbol{\chi};t-\tau)\varphi(\boldsymbol{\chi},\tau)\right\}d\Gamma(\boldsymbol{\chi})d\tau$$

where "*id*" denotes instantaneous displacement discontinuity. $\sigma^{id}{}_{ijk}$ and $p^{id}{}_{k}$ are the stress tensor and the pore pressure caused by an instantaneous displacement discontinuity, respectively. D_k is the strength (magnitude) of the displacement discontinuity in *k* direction. Other terms have the same meanings. It can be seen that temperature is calculated separately while pore pressure and stress are fully coupled.

The numerical procedure solving the above integral equations for the unknown DD's and fluid/heat sources consist of using a boundary collocation technique, e.g., (Ghassemi and Zhang, 2006). The problem boundary is divided into a number of elements (J) and fictitious forces and fluid/heat sources are distributed over each element in space and time using a desired shape function such that the sum of their effects satisfies the prescribed boundary conditions. In the present implementation, it is assumed that boundary elements are straight segments with collocation points located at the centre of each element. The variation of DD's is assumed to be constant over time also. A computer program is developed based on the above procedures and is applied below.

EXAMPLE

As a first example, consider the problem of injection into a reservoir to study the influence of thermal stress on injection well fracturing. The current approach assumes that the well and fractures that form are continuously pressurized and cooled by the cold water. If the injection condition is such that the well is fractured as it is cooled and pressurized, the cooled zone will evolve in size and geometry as the fracture propagates. Currently, this process is simulated using a suddenly cooled and pressurization fracture without considering the condition for fracture propagation. We will focus on the pore pressure and stress distribution around the fracture to assess rock fracturing and contribution to seismicity.

Initially, when the effective tangential stress around the well exceeds the tensile strength of the formation, a short fracture forms in the direction of the major in-situ stress, and extends from the well, as shown in Figure 1.

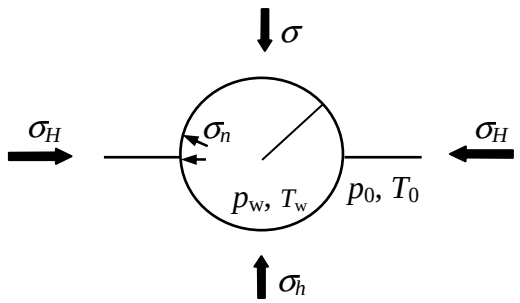

Figure 1. Hydraulic fracturing of an injection well.

Consider the injection water and rock temperature to be 80°C and 280°C, respectively, with a well radius of $R = 0.1m$. Assume the current length of the fracture is $0.5R$. In order to examine the impact of the thermally induced stress only, the mechanical and hydraulic loadings are not considered. That is, no in-situ or boundary stresses and pressures are applied. Figure 2 plots the temperature field at time = 28 hrs. As shown, the cooled region around the well and the short fracture is nearly circular. Figure 3 shows the difference between the major and minor principal stresses induced by cooling. One can see the differences of thermally induced stresses in two principal directions are very small in the cooled region outlined by the dashed ellipse. Therefore, the magnitudes of thermally induced stresses (which

reduce the in-situ stresses) are nearly uniform in all directions. As a result, when the in-situ stresses are applied, the direction of the minor in-situ stress remains the same as the initial one in the formation. And consequently the orientation of any new fractures will also remain the same.

Now, consider another case when the fracture has extended a greater distance from the well. In this example, the length of the fracture is considered to be 14*R*. The cooled region becomes more elongated as shown in Figures 4, and 5. At time = 28 hrs, the temperature of the region shown in the dashed ellipse is approximately 100°C. Figure 6 plots the difference between major and minor principal stress induced by cooling. The plot indicates that the difference between the magnitudes of thermally induced stresses parallel and perpendicular to the fracture is much larger in the cooled region than outside. That is, in the elliptical cooled region the thermoelastic reduction of the in-situ stress parallel to the fracture ($\Delta\sigma_H$) is much greater than the thermoelastic stress reduction perpendicular to the fracture ($\Delta\sigma_h$). Let *a* be the length of the long axis of the ellipse in the direction of σ_H, and *b* the length of the short axis in the direction of σ_h, then the expressions for $\Delta\sigma_H$ and $\Delta\sigma_h$ in the uniformly cooled region are given by (Perkins and Gonzalez, 1985):

$$\Delta\sigma_H = \frac{1}{(1+b/a)} \cdot \frac{E\beta_s \Delta T}{3(1-\nu)}$$

$$\Delta\sigma_h = \frac{b/a}{(1+b/a)} \cdot \frac{E\beta_s \Delta T}{3(1-\nu)} \qquad (13)$$

According to Equations (13), on the crack surface where the ΔT is -200°C, the difference between $\Delta\sigma_H$ and $\Delta\sigma_h$ can be 78 MPa for an ellipse with *b/a* = 0.01, and 56 MPa for *b/a* = 0.1. The value could be lower inside the formation where the temperature change (ΔT) is not as high as at the crack surface.

The impact of cooling on the net stress state within the elongated cooled region is illustrated by the following example using the same well and fracture geometries as before. Assume the major and minor in-situ stresses and pore pressure are 40 MPa, 10 MPa, and 10 MPa, respectively, the direction of the minor principal stress is perpendicular to the fracture. The normal stress and pressure applied on the well boundary and fracture surfaces are 10 MPa and 10MPa, respectively. Thermal loading remains the same with previous example, i.e., a ΔT of 200°C. Therefore, the temperature field and cooled region at time = 28 hrs is the same as the one shown in Figure 5. The pore pressure distribution after 2 and 28 hrs of cooling is shown in Figures 7 and 8, respectively. It can be seen the cooling induces significant decreases in pore pressure in a relatively large area. Near the fracture, the hydraulic boundary condition restores the pore pressure after the cooling front has passed this area. The pore pressure reduction has a stabilizing effect with respect to shear failure. This effect is ephemeral, as the cooling effect will be dominated by the pressure effect.

The difference between the total (in-situ plus induced) major and minor principal stresses is plotted in Figure 9. It can be seen that the difference between the total major and minor principal stresses is greatly reduced in the cooled region. Note that the original difference between the principal stresses was 30 MPa everywhere, and with cooling it is reduced to less than 10 MPa in most areas of the cooled region. This indicates that in a sufficiently cooled region, the stress parallel to the fracture can become less than that perpendicular to the fracture. As a result, secondary fractures would form perpendicular to the primary main fracture as shown in Figure 10 (Perkins and Gonzalez, 1985). Formation of these fractures can be accompanied by micro-seismic events.

There are also areas where the difference between the principal stresses increases. These include points in the vicinity of the wellbore and in areas near the fracture tips, where stress singularity exists, as well as areas off the fracture plane beyond the cooled area (near the corners of the plotted region). Higher shear stresses in these areas can cause rock failure in shear and induced micro-seismicity.

Table 1. Input parameters.

Parameter			
E	Elastic modulus	3.75×10^4	MPa
ν, ν_u	Poisson's ratio	0.25, 0.33	
K_r	Solid bulk mod.	4.5×10^4	MPa
K_s	Fluid bulk	2.5×10^3	MPa
B	Skempton's coef.	0.815	
ρ_r	Rock density	2650	kg/m^3
ρ_w	Water density	1000	kg/m^3
C_r	Rock heat cap.	790	J/(kg C)
C_w	Water heat cap.	4200	J/(kg C)
κ	Thermal diff.	5.1 E -6	m^2 /sec
β_f	Fluid exp. coef.	3.00×10^{-4}	1/°C
β_s	Rock exp. coef.	2.4 E -5	m / C
k	Permeability	4.053×10^{-7}	Darcy

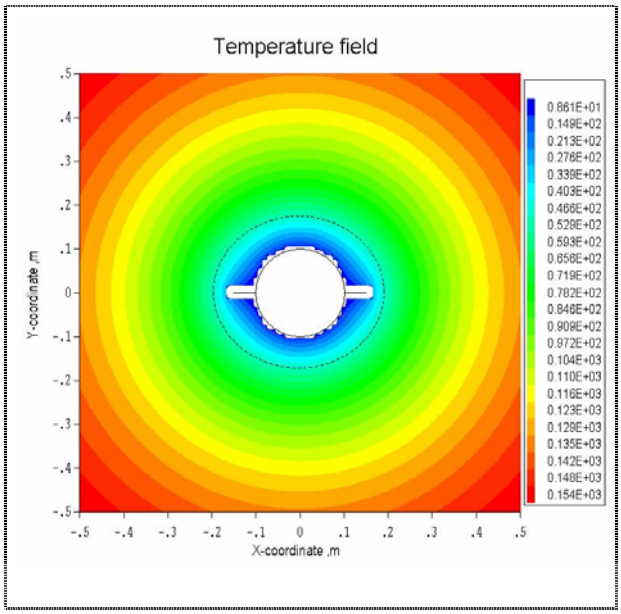

Figure 2. Temperature field around an injection well and a short fracture.

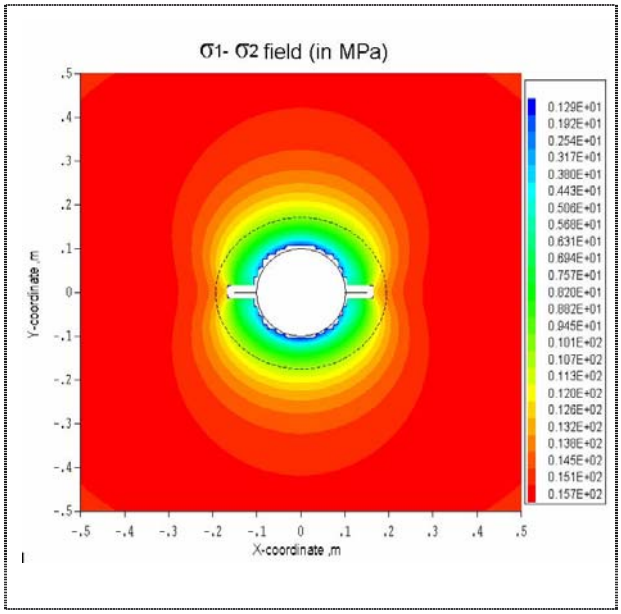

Figure 3. Difference between thermally-induced principal stresses around an injection well with a short fracture.

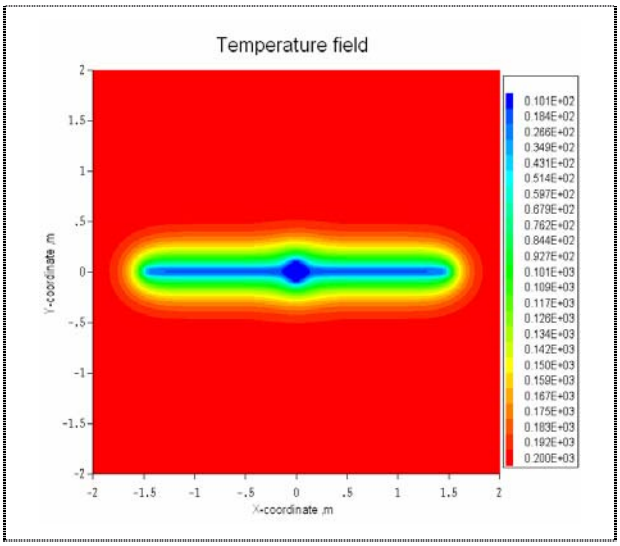

Figure 4. Temperature field around the well/crack after 2 hrs.

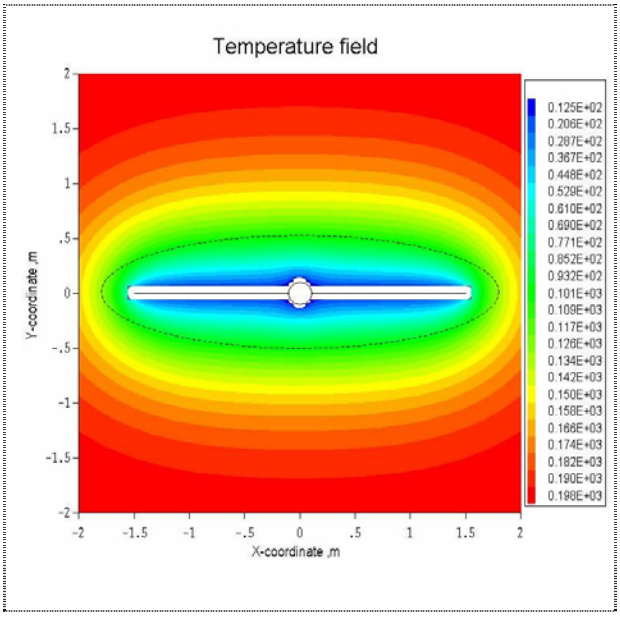

Figure 5. Temperature field around an injection well and a longer fracture after 28 hrs.

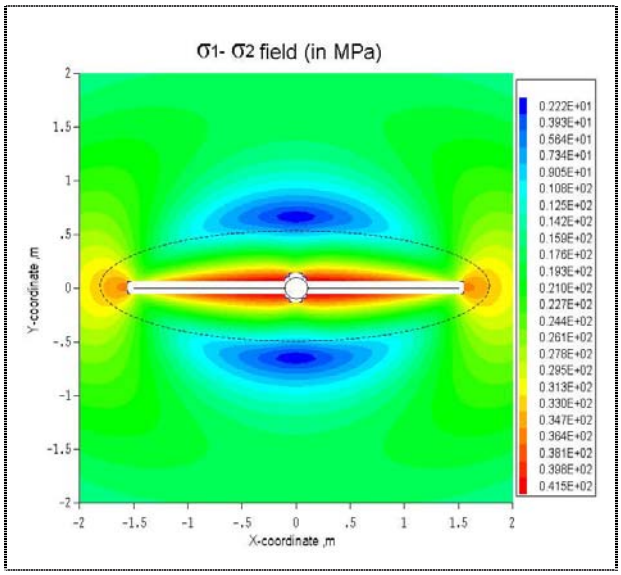

Figure 6. The difference between thermally-induced principal stresses around the fracture after 28 hrs.

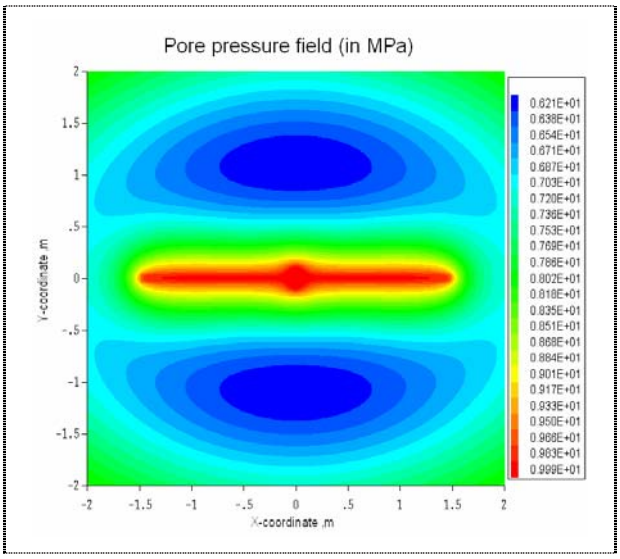

Figure 8. Pore pressure field around the cooled crack after 28 hrs.

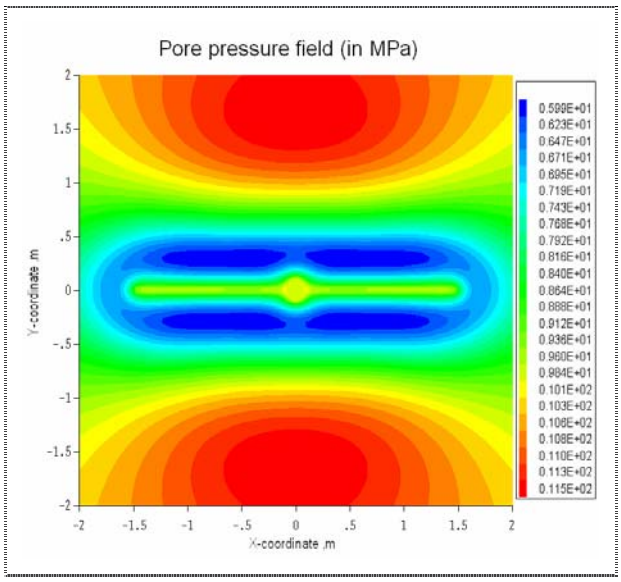

Figure 7. *Pore pressure distribution around the fracture after 2 hrs.*

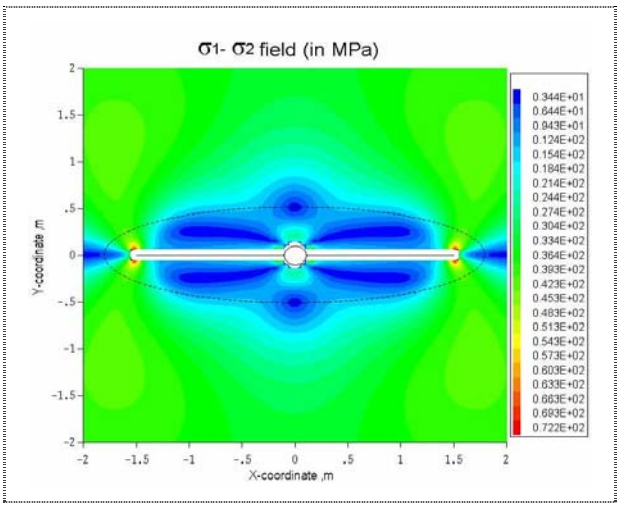

Figure 9. Difference between principal stresses around an injection well and a longer fracture after 28 hrs.

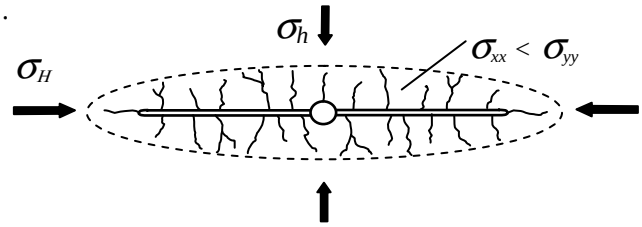

Figure 10. Formation of secondary fractures within cooled region.

CONCLUSIONS

A 2D porothermoelastic displacement discontinuity boundary element model has been used to investigate thermally-induced pore pressure and stresses around a fracture in low permeability rock. Cooling reduces the pore pressure which has a stabilizing effect with respect to shear failure of intact rock and slip on pre-existing cracks. Thermally-induced stresses in the cooled region cause formation of new, secondary cracks that can generate seismic events. Large cooling causes these to propagate perpendicular to the original fracture as the difference between in-situ stress components is reduced in the cooled zone. Also, regions of enhanced shear stress occur away from the main cooled zone, where rock failure or slip on preexisting cracks may occur. A rock failure analysis can provide additional insights regarding each mechanism and the expected types of rock failure, and associated micro-seismicity. A more realistic assessment would also consider non-uniform cooling of the rock and will be reported in the future.

ACKNOWLEDGEMENTS

This project was supported by the U.S. Department of Energy Office of Energy Efficiency and Renewable Energy under Cooperative Agreement DE-FG36-06GO95002. This support does not constitute an endorsement by the U.S. Department of Energy of the views expressed in this publication.

REFERENCES

Brady, J.L., Withers, R.J., Fairbanks, T.D., and Dressen, D., (1994), Microseismic monitoring of hydraulic fractures in Prudhoe Bay. SPE 28553.

Cornet, F.H. and Jianmin, Y., (1995), Analysis of induced seismicity for stress field determination and pore pressure mapping. *Pure and Applied Geophys*., **145**(3/4), 677-700.

Crouch, S.L., and Starfield, A.M., (1983), Boundary element methods in solid mechanics, Allen Unwin, NY.

Foulger, G.R, Julian, B.R., Hill, D.P., Pitt, A.M., Malin, P., and Shalev, E., (2004). Non-double-couple micro-earthquakes at Long Valley Caldera provide evidence for hydraulic fracturing. *J. Volc. Geotherm. Res.*, **132**, 45-71.

Ghassemi, A. and Roegiers, J.-C., (1996), A three-dimensional poroelastic hydraulic fracture simulator using the displacement discontinuity method. Proc. 2nd North American Rock Mech. Symposium, Montreal, Ca, **1**, 982-987.

Ghassemi, A., Zhang, Q., (2006), Poro-thermoelastic response of a stationary crack using the displacement discontinuity method. *ASCE Journal of Engineering Mechanics*, **132**(1), 26-33.

Gutierrez-Negrin L.C.A., Quijano-Leon J.L., (2003), Analysis of seismicity in the Los Humeros, Mexico, geothermal field. Geothermal Resources Council Transactions, **28**.

Nygren, A., and Ghassemi, A., (2006), Coupled Poroelastic and Thermoelastic Effects of Injection into a Geothermal Reservoir. 40th U.S. Rock Mech. Symp., Golden, CO.

Nygren, A., and Ghassemi, A., Cheng A.H.-D., (2005), Effects of cold-water injection on fracture aperture and injection pressure. GRC Annual Conf., Reno, Nevada.

Peasron, C., (1981), The relationship between micro-seismicity and high pore pressure during hydraulic stimulation experiments in low permeability rocks. *J. Geophy. Res*., 86, B9, 7855.

Perkins, T.K., and Gonzalez, J.A., (1985), The effect of thermoelastic stresses on injection well fracturing", SPE 11332.

Pine R. J., and Batchelor, A.S., (1984), Downward migration of shearing in jointed rock during hydraulic injections, *Int. J. Rock Mech. Min. Sci. & Geomech*. Abstr. **21**(5), 249-63.

Palciauskas V.V., and Domenico P.A., (1982), Characterization of drained and undrained response of thermally loaded repository rocks, *Water Resour. Res*. 18: 281-290.

Vandamme, L., Talebi, S., and Youmg, R.P., (1994), Monitoring of a hydraulic fracture in a South Saskatchewan oil field. *J. Can. Pet. Tech*, 33, 27.

Warpinski, N.R., Wolhart, S.L., and Wright, C.A., (2001), Analysis and prediction of microseismicity induced by hydraulic fracturing. SPE 71649.

Warpinski, N.R., Wright, T.B., Uhl, J.E., Engler, B.P., Drozda, P.M., and Pearson, R.E., (1996), Micro-seismic monitoring of the B-Sand hydraulic fracture experiment at DOE/GRI Multi-site Projects, SPE 36450.